MÜNSTER UNIVERSITY OF APPLIED SCIENCES
Department of Electrical Engineering and Computer Science

Bachelor Thesis

KALMAN FILTERING APPLIED TO ORIENTATION ESTIMATION IN HUMAN BODY MOTION ANALYSIS

Supervisors:

Author:

Robin Weiß

Prof. Dr.-Ing. Peter Glösekötter

Ph.D. Alberto Olivares Vicente

Prof. Dr. med. Kai Bötzel

A thesis submitted in partial fulfilment of the requirements for the degree of Bachelor of Science in Electrical Engineering

April 2015

Statement of Authorship

I hereby certify that this bachelor thesis has been composed by myself, and describes my own work, unless otherwise acknowledged in the text. All references and verbatim extracts have been quoted, and all sources of information have been specifically acknowledged. It has not been accepted in any previous application for a degree.

Granada, 8th April 2015

Robin Weiß

Preface

This thesis was submitted in partial fulfilment of the requirements for the degree of Bachelor of Science in Electrical Engineering. It describes the implementation of a new Kalman filter based orientation algorithm to improve the estimation of orientation angles by means of inertial sensors.

I took part in the joint research project "Human Body Motion Analysis of Patients with Neurodegenerative Diseases by Means of Inertial Sensors" between the Research Centre for Information and Communications Technologies of the University of Granada (CITIC-UGR), Spain, and the Department of Neurology of the Klinikum Großhadern, which is part of the Ludwig Maximilian University of Munich, Germany. The goal of the overall project was to obtain several gait parameters by wearable inertial sensors and validate them against conventional methods such as force plates and cameras in combination with visual markers. Physicians and medical researchers are interested in this approach of body motion analysis, as it can assist the diagnosis of neurodegenerative diseases such as Parkinson's. Prior to this thesis I completed a three-months internship at the CITIC-UGR in which I worked on the synchronisation of a force measuring plate and inertial sensors within the above-mentioned project.

Münster University of Applied Sciences

Department of Electrical Engineering and Computer Science

Abstract

Kalman Filtering Applied to Orientation Estimation in Human Body Motion Analysis

by Robin Weiß

Lorem ipsum dolor sit amet, consectetuer adipiscing elit. Etiam lobortis facilisis sem. Nullam nec mi et neque pharetra sollicitudin. Praesent imperdiet mi nec ante. Donec ullamcorper, felis non sodales commodo, lectus velit ultrices augue, a dignissim nibh lectus placerat pede. Vivamus nunc nunc, molestie ut, ultricies vel, semper in, velit. Ut porttitor. Praesent in sapien. Lorem ipsum dolor sit amet, consectetuer adipiscing elit. Duis fringilla tristique neque. Sed interdum libero ut metus. Pellentesque placerat. Nam rutrum augue a leo. Morbi sed elit sit amet ante lobortis sollicitudin. Praesent blandit blandit mauris. Praesent lectus tellus, aliquet aliquam, luctus a, egestas a, turpis. Mauris lacinia lorem sit amet ipsum. Nunc quis urna dictum turpis accumsan semper.

Contents

List of Figures

List of Tables

Abbreviations

ARW   Angle random walk

CITIC-UGR   Research Centre for Information and Communications
                  Technologies of the University of Granada

EKF   Extended Kalman filter

IMU   Inertial measurement unit

LTSD   Long term spectral detector

MARG sensors   Magnetic, angular rate, and gravity sensors
MEMS   Microelectromechanical systems
MIMU   Magnetic inertial measurement unit

RMSE   Root-mean-square error

Notation

a   Three-dimensional acceleration vector

b   Position vector in a three-dimensional vector space

B   Control matrix that relates the control input to the state **x**

$\mathbf{C}_{bn}$ Transformation matrix transforming a position vector from the body frame to the navigation frame

$\mathbf{C}_{nb}$ Transformation matrix transforming a position vector from the navigation frame to the body frame

d   Desired filter response of a linear discrete-time filter

e   Error signal of a linear discrete-time filter

F   Three-dimensional force vector

h   Functional denoting the *non-linear* measurement matrix function of a discrete dynamical system

H   Measurement sensitivity matrix defining the linear relationship between the state of the dynamical system and the measurements that can be made

k   Discrete time normalised to sampling interval (sample number), $k \in \mathbb{N}^0$

K	Weighting factor
$\mathbf{K}$	Kalman gain matrix
m	Mass
n	Discrete time
$\mathbf{\Omega_{E\rightarrow E}}$	Function that transforms a position vector $\mathbf{b}$ in the vector space $\mathbf{E}$ into the vector $\mathbf{b}'$ in the vector space $\mathbf{E}'$
$\mathbf{P}$	Covariance matrix of state estimation uncertainty
ϕ	Roll angle that determines the rotation around the x-axis
$\boldsymbol{\phi}$	Functional denoting the *non-linear* transition matrix function of a discrete dynamical system
$\mathbf{\Phi}$	State transition matrix of a discrete linear dynamical system
ψ	Yaw angle that determines the rotation around the z-axis
$\mathbf{Q}$	Covariance matrix of process noise in the system state dynamics
$\mathbf{R}$	Covariance matrix of observational (measurement) uncertainty
μ	Mean value of conditional probability density
σ^2	Variance
σ	Standard deviation
t	Continuous time
$\mathbf{T}$	Transformation matrix
θ	Pitch angle that determines the rotation around the y-axis
u	Nominal velocity
$\mathbf{v}$	Measurement noise vector

w	Noise term
$w_0, w_1, w_2, \ldots$	Impulse response of a linear discrete-time filter
$\mathbf{w}$	Process noise vector
x	One-dimensional location
$\hat{x}$	Estimate of x
x, y, z	Axes of the fixed navigation frame
X, Y, Z	Axes of the moving body frame
$\mathbf{x}$	State vector of a linear dynamical system
$\mathbf{x}_k$	The kth element of a sequence $\ldots$, $\mathbf{x}_{k-1}$, $\mathbf{x}_k$, $\mathbf{x}_{k+1}, \ldots$ of vectors
$\hat{\mathbf{x}}$	Estimate of the state vector of a linear dynamical system
$\hat{\mathbf{x}}_k^-$	A priori estimate of $\hat{\mathbf{x}}$, conditioned on all prior measurements except the one at time t_k
$\mathbf{y}$	Observation vector of a dynamical system
$y(0), y(1), y(2), \ldots$	Time series that serves as input to a linear discrete-time filter
z^{-1}	Unit-delay
$\mathbf{z}$	Vector of measured values

Chapter 1

Introduction

Orientation estimation of the human body assisted by inertial sensors has become an integral part of medical diagnosis, therapy techniques, and rehabilitation as it provides an objective means of monitoring and assessing human body motion. The progressive miniaturisation of unobtrusive wearable inertial and magnetic sensors has made them more acceptable to patients and has consequently lead to an increasingly pervasive adoption for medical applications [7].

For the application in health care accurate orientation estimates are crucial. A high degree of precision based on data from miniaturised sensors necessitates adequate signal processing, in order to mitigate the influence of disruptive factors such as bias instability and noise. That is, mathematically modelling the movement of interest, adaptive filtering, and sensor fusion.

1.1 Motivation

1.2 Goals

The goal of this thesis was implementing a new Kalman filter based orientation algorithm proposed by Bennett et al. in [4] to improve the estimation of orientation angles of the human leg by means of inertial sensors. The filter algorithm should be implemented using MATLAB® and validated against existing algorithms by comparing their respective root-mean-square error (RMSE). An existing system for human body motion analysis called GaitWatch was available so that no new hardware had

to be developed to gather the movement data. A detailed description of the Device is found at the end of Chapter 2. The data was gathered at Department of Neurology of the Klinikum Großhadern, Munich. The subject stood in front of the force plate. Then, the GaitWatch and force plate record was started and the subject made a step onto the force plate. After standing upright for a variable time of two to ten seconds the subject left the force plate, made a few steps, turned left, and stopped in front of it again. This sequence was repeated ten times.

1.3   Methodology

At first Fudamentals..

As additional means to communicate with my supervisor and enable him to follow the progress of the project at any time we used Pivotal Tracker, a tool for agile project management and GitHub, a repository hosting service based on the distributed version control system Git. This thesis was written in the document markup language LaTeX.

1.4   Document structure

Subsequent to the previous introductory overview of the subject and the definition of the project objectives, this chapter ends with a description of the state of the art. Chapters 2 to 4 outline the necessary fundamentals of MARG sensors, orientation estimation and digital filters, respectively. The actual implementation of the Kalman filter, including a prior theoretical design is given in Chapter 5, in which also the results are presented and discussed. Finally, Chapter 6 concludes and proposes possible future work.

1.5   State of the Art

There are several research works in the literature dealing with orientation estimation by means of inertial sensors. Kalman filters have been used successfully to improve these angle estimations. The state of the art at the commencement of the project is described below. Subsequently, current attempts to revolutionise medical research assisted by inertial sensors are presented.

1.5.1 Kalman Filtering in Orientation Estimation

Considering the fact that inertial and magnetic field sensors are used to establish objective body motion parameters that affect medical diagnosis, therapy, and rehabilitation, the necessity of a high level of accuracy becomes obvious. In order to obtain precise orientation estimates from sensor data it is essential to mitigate the effects of measurement noise and to combine the advantages of different sensors through sensor fusion. Therefore, a wide variety of Kalman filter algorithms have been developed in the literature.

Many did not consider linear acceleration.

Due to human motion usually being subject to change, Olivares Vicente implemented a *gated Kalman filter* in [8]. They modelled linear acceleration during intense motion as noise and improved the performance of the Kalman filter by dynamically adjusting the variance of both the process and measurement noise, according to the motion intensity. Therefore they applied a long term spectral detector (LTSD) and set the variance between two predefined values. Then, the gated Kalman filter fused information from the accelerometer and the gyroscope signals. Thus, they improved the adapting capability of the filter and consequently the precision of the orientation estimation.

Bennett et al. demonstrated in [4] that accelerometer angle estimates are inaccurate for typical motions of the leg. They affirmed the need to decouple the acceleration due to motion from the acceleration due to gravity, since the former cannot be neglected during fast motions. Therefore, they deployed a kinematic model of the leg to determine the acceleration that occurs due to motion and corrected the acceleration signal accordingly. An extended Kalman filter fused the corrected acceleration data with measurements of a gyroscope during motion. Their method improved upon the raw accelerometer method during motion and at rest by an 83% smaller RMSE.

1.5.2 MARG Sensors in Medical Research

MARG sensors can be found in smart phones, fitness trackers, and other wearable devices. With increasing capability of body sensor networks and wearable computing, they have become prevalent in research environments for estimation and tracking of human body motion [4]. They

are used in activity monitoring [9][10][11], rehabilitation [12][13], sports training [14][11], and localisation [15][16].

The number of smartphones across the globe is predicted to surpass two billion in 2016 [17], of which most come equipped with MARG sensor technologies. Recently, large companies have developed software that takes advantage of the associated potential to revolutionise medical research.

In March 2015, Apple Inc. announced a platform-independent, open source software framework called ResearchKit [18] that, amongst others, takes advantage of the MARG sensors in the iPhone to track movement of patients in daily life. Thus medical researchers obtain robust data with far more regularity than it was possible when patients complete tasks at hospitals or other research facilities in irregularly intervals. Moreover, according to Apple Inc. ResearchKit simplifies recruiting participants from all over the world, which results in a more varied study group that provides a more useful representation of the population. Together with the University of Rochester and Sage Bionetworks they announced the iPhone app 'mPower', which measures balance and gait of parkinson patients to help researchers better understand how various symptoms are connected to Parkinson's disease.

In August 2014, the Michael J. Fox Foundation for Parkinson's Research and Intel Corporation [19] announced a collaborative research study on objective measurement of Parkinson symptoms. They aim to collect movement data of thousands of patients twenty-four seven at over 300 samples per second by means of unobtrusive wearable devices and store them on a big data analytics platform. The data platform, deployed on a cloud infrastructure, supports an analytics application that processes the data and detects changes in real time. Thus, by detecting anomalies, the progression of the disease can be measured objectively without the need for scientists to focus on the underlying computing technologies. Physicians and researchers are intended to have access to the data as well as be able to submit their own anonymised patient data for analysis. According to [19] the correlation of data that quantifies symptoms such as slowness of movement, tremor, and sleep quality with molecular data could advance drug development and provide a deeper insight into the clinical course of Parkinson's disease.

Chapter 2

MARG Sensors

MARG sensors is a collective term for magnetic, angular rate, and gravitational sensors that encompasses inertial sensors, as well as magnetic field sensors, also referred to as magnetometers. Inertial sensors generally fall into two categories: instruments sensing linear inertial displacement (accelerometers) and rotational inertial rate sensors (gyroscopes). They can be applied in various contexts to quantify vibration, motion, and shock [1]. Particularly, the development of microelectromechanical systems (MEMS) opened up many medical applications as mentioned in the previous Section 1.5.2. This chapter compiles the functional principles of MARG sensors and introduces inertial measurement units (IMUs) as a combination of those. At the end of the chapter the aforementioned GaitWatch device is described in detail.

2.1 Accelerometers

Accelerometers measure the acceleration of an object relative to an inertial frame. Since acceleration cannot be measured directly, the force exerted to a reference mass is obtained and the resultant acceleration is computed according to Newton's second law $\mathbf{F} = m \cdot \mathbf{a}$, where $\mathbf{F}$ denotes the three-dimensional force vector, m the mass, and $\mathbf{a}$ the three-dimensional acceleration vector. Usually, an accelerometer consists of a small proof mass connected via a spring to the case of the instrument. The proof mass is displaced by Δx with respect to the case, when the instrument experiences a certain acceleration along its sensitive axis. Disregarding drag force, the displacement is directly proportional to the force exerted
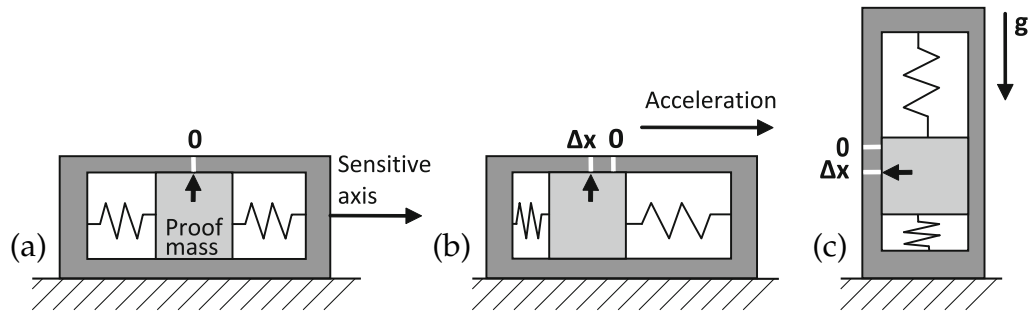
Figure 2.1: A mass-and-spring accelerometer under different conditions: (a) at rest or in uniform motion, (b) accelerating, and (c) at rest from [1].

by the mass and thus to the acceleration. Therefore, by measuring the displacement of the proof mass the acceleration can be obtained. Figure 2.1 shows the displacement Δx of the mass in respect to the case of the instrument for three different conditions: (a) at rest or in uniform motion, (b) accelerating, and (c) at rest. In cases where the three-dimensional vector of the acceleration is required, three single-axis accelerometers are used. Although a mutually orthogonal mount is common practice, any non-coplanar arrangement is acceptable, as long as the angle between the sensitive axis are known [1].

2.2   Gyroscopes

Gyroscopes, also called angular rate sensors, measure angular velocity and are based on the Coriolis Effect. By integrating the angular velocity the rotation angle is obtained [8].

2.3   Magnetometers

Magnetometers measure the strength and the direction of the magnetic field in a point in space, using the relationship between magnetic fields, movement and induced currents [8].

2.4 Inertial Measurement Units

Devices using a combination of accelerometers and gyroscopes to measure the orientation of a rigid body with up to six degrees of freedom are referred to as IMUs. If they include additional magnetometers they are termed magnetic inertial measurement units (MIMUs) and can obtain the orientation of the body with up to nine degrees of freedom, whereby the number of degrees of freedom states the number of independent motions, with respect to a reference frame, that are allowed to the body in space.

MIMUs are portable and relatively inexpensive. They can be easily attached to the body and thus allow non-clinical longterm application. Their drawbacks are complex calibration procedures and drift behaviour over time, depending on intensity and duration of the measurement interval. Hence, in order to maintain a satisfactory degree of precision, periodical recomputation of the calibration parameters is required [8].

2.5 The GaitWatch

The above mentioned GaitWatch device we used to gather the movement data was designed to monitor the motion of patients while attached to the body. It was developed at the Department of Neurology of the Ludwig-Maximilians University in Munich, Germany, in association with the Department of Signal Theory, Telematics and Communications of the University of Granada, Spain. The system is composed of a set of embedded magnetic and inertial sensors wired to a box containing a microcontroller. This microcontroller is in charge of collecting data from the embedded box sensors, as well as from the external measurement units, and storing them on a memory card. The various units are placed at the patient's trunk, arms, thighs, and shanks as shown in Figure 2.2. The components of the three different kinds of subunits are described below:

- Type A – thighs and shanks:

  IMU Analog Combo Board with 5 Degrees of Freedom [20], containing an IDG500 biaxial gyroscope, from which only y-axis is actually used, with a measurement range of $\pm 500\,°/s$ [21] and a $\pm 3\,g$ triaxial accelerometer, ADXL335 [22].

- Type B – arms:
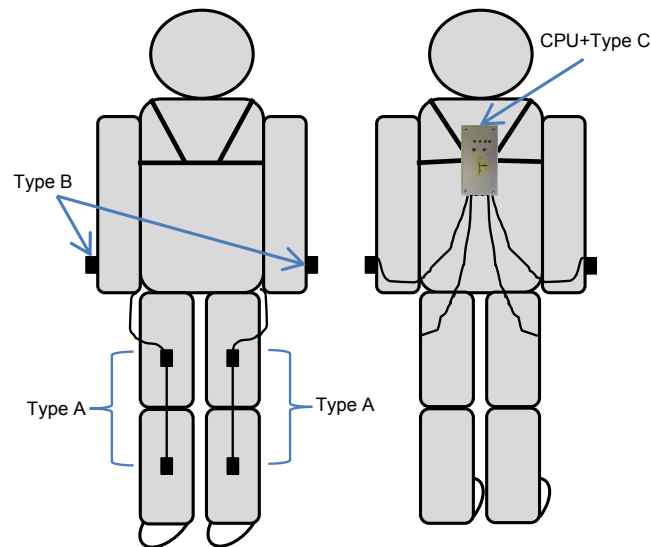
Figure 2.2: Placement of the GaitWatch components at the body from [2].

IDG500 biaxial gyroscope with a measurement range of ±500 °/s [21].

- TYPE C – trunk:

  ADXL345 triaxial accelerometer with a programmable measurement range of ±2/±4/±8/±16 g [23], IMU3000 triaxial gyroscope with a programmable measurement range of ±250/±500/±1000/±3000°/s [24], Micromag3 triaxial magnetometer with a measurement range of ±11 Gauss [25], AL-XAVRB board containing an AVR ATxmega processor [26].

Chapter 3

Orientation Estimation

In the motion monitoring field and especially in aircraft navigation the position of the coordinate frame of the body, with respect to a reference coordinate frame, is known as attitude, which is used as a synonym of orientation. There are different approaches to compute attitude estimates from magnetic and inertial data. This chapter explains their pros and cons and introduces sensor fusion as a means to mitigate the drawbacks of each approach. Beforehand, two main mathematical constructs used to express attitude – Euler angles and quaternions – are described.

3.1 Euler Angles

Euler angles are one of several ways to describe the orientation of an object and its associated body frame in three-dimensional Euclidean space, with respect to the navigation frame, i.e. the reference frame. They represent a sequence of three elemental rotations about the axes of the coordinate system, defined as follows:

- The *roll* angle ϕ determines the rotation around the x-axis with a range $-\pi < \phi \leq \pi$.

- The *pitch* angle θ determines the rotation around the y-axis with a range $-\frac{\pi}{2} \leq \theta \leq \frac{\pi}{2}$.

- The *yaw* angle ψ determines the rotation around the z-axis with a range $-\pi < \psi \leq \pi$.

Figure 3.1 depicts the rotation about the axes z, y', Z by ψ, θ, ϕ, respectively, according to the Tait-Bryan convention. The colour blue indicates the orientation before and the colour red the orientation after the rotation. In contrast to extrinsic rotations, where the three elemental rotations may occur either about the axes of the original coordinate system, the Tait-Bryan rotations are intrinsic rotations that occur about the axes of the rotating coordinate system, which changes its orientation after each rotation.
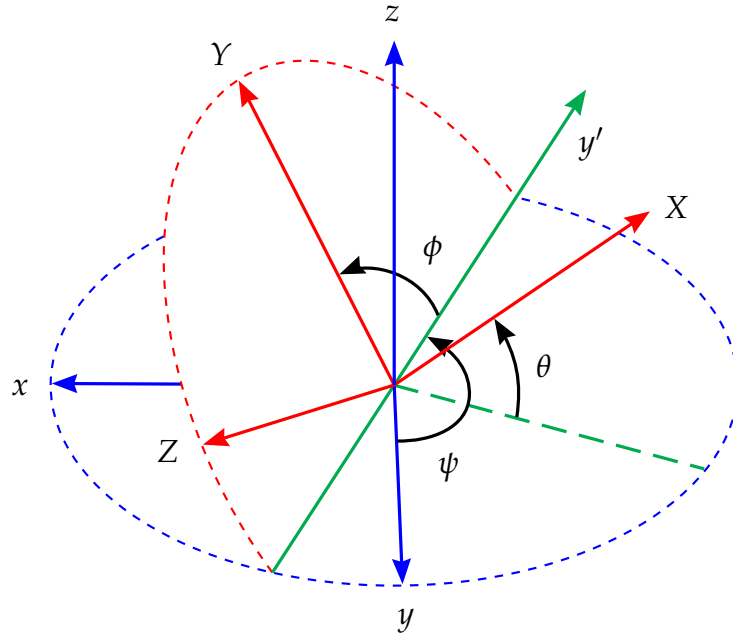
Figure 3.1: Representation of the body frame (red) with respect to the navigation frame (blue). The body frame was rotated, by the Euler angles ψ, θ, ϕ about the axes z, y', X, respectively. Adapted from [3].

Euler angles are a simple and intuitive means to represent rotations in three-dimensional space. However, for the above mentioned parameterisation they have singularities at values of $\theta = n\pi$ for $n \in \mathbb{Z}$. At these points a rotation about the X-axis and the z-axis constitute the same motion, which results in the loss of one degree of freedom and makes changes in ϕ and ψ indistinguishable. This phenomenon is called *gimbal lock*. The usage of *quaternions* instead of Euler angles avoids the problem of gimbal locks.

3.2 Transformation Matrices

Coordinates representing a point in one coordinate system can be transformed to another. Such a linear transformations can be expressed as multiplication of a matrix with the coordinate vector that is to be transformed. Let $\mathbf{E}$ denote the orthonormal basis $\{x, y, z\} \in \mathbb{R}^3$ and let $\mathbf{E}'$ denote the orthonormal basis $\{X, Y, Z\} \in \mathbb{R}^3$. Furthermore, let $\mathbf{b}$ denote the position vector of a point in three-dimensional Euclidean space. The coordinate transformation from $\mathbf{E}$ to $\mathbf{E}'$ is denoted $\Omega_{\mathbf{E} \to \mathbf{E}'} : (b_1, b_2, b3) \mapsto (b1', b2', b3')$. Then, the transformation from $\mathbf{b}$ to $\mathbf{b}'$ is given by

$$\mathbf{b}' = \Omega_{\mathbf{E} \to \mathbf{E}'}(\mathbf{b}) = \mathbf{T}\mathbf{b}, \tag{3.1}$$

where $\mathbf{T}$ is the transformation matrix.

To transform the coordinate vector from the navigation frame to the body frame, according to the common aerospace rotation sequence mentioned above and the Nort-East-Down system (NED), the transformation matrix C_{nb} is given by

$$
\begin{aligned}
\mathbf{C}_{nb} &= \mathbf{T}_x(\phi)\mathbf{T}_y(\theta)\mathbf{T}_z(\psi) \\
&= \begin{bmatrix} 1 & 0 & 0 \\ 0 & \cos\phi & \sin\phi \\ 0 & -\sin\phi & \cos\phi \end{bmatrix} \begin{bmatrix} \cos\theta & 0 & -\sin\theta \\ 0 & 1 & 0 \\ \sin\theta & 0 & \cos\theta \end{bmatrix} \begin{bmatrix} \cos\psi & \sin\psi & 0 \\ -\sin\psi & \cos\psi & 0 \\ 0 & 0 & 1 \end{bmatrix} \\
&= \begin{bmatrix} \cos\theta\cos\psi & \cos\theta\sin\psi & -\sin\theta \\ \sin\phi\sin\theta\cos\psi - \cos\phi\sin\psi & \sin\phi\sin\theta\sin\psi + \cos\phi\cos\psi & \sin\phi\cos\theta \\ \cos\phi\sin\theta\cos\psi + \sin\phi\sin\psi & \cos\phi\sin\theta\sin\psi - \sin\phi\cos\psi & \cos\phi\cos\theta \end{bmatrix}
\end{aligned} \tag{3.2}
$$

Plugged in Equation 3.1 ($\mathbf{T} = \mathbf{C}_{nb}$) the left multiplications of the matrices $\mathbf{T}_x(\phi), \mathbf{T}_y(\theta), \mathbf{T}_z(\psi)$ to the vector $\mathbf{b}$ represent the coordinate rotations about the single axes x, y, z, respectively. That is, the orthogonal projection onto the axes of the coordinate system, which result from the respective two-dimensional rotation of ϕ, θ, ψ about the axes x, y, z, is computed. This is illustrated in Figure 3.2. The single matrices $\mathbf{C}_{bn}$ and $\mathbf{C}_{nb}$ are also known as direction cosine matrices, since their elements are the cosines of the unsigned angles between the body-fixed axes and the axes of the navigation frame. The form stated here is already simplified. The matrix $\mathbf{C}_{bn}$ for transforming the coordinate vector from the body frame to the navigation frame is given by

$$\mathbf{C}_{bn} = \begin{bmatrix} \cos\theta\cos\psi & \sin\phi\sin\theta\cos\psi - \cos\phi\sin\psi & \cos\phi\sin\theta\cos\psi + \sin\phi\sin\psi \\ \cos\theta\sin\psi & \sin\phi\sin\theta\sin\psi + \cos\phi\cos\psi & \cos\phi\sin\theta\sin\psi - \sin\phi\cos\psi \\ -\sin\theta & \sin\phi\cos\theta & \cos\phi\cos\theta \end{bmatrix} \tag{3.3}$$
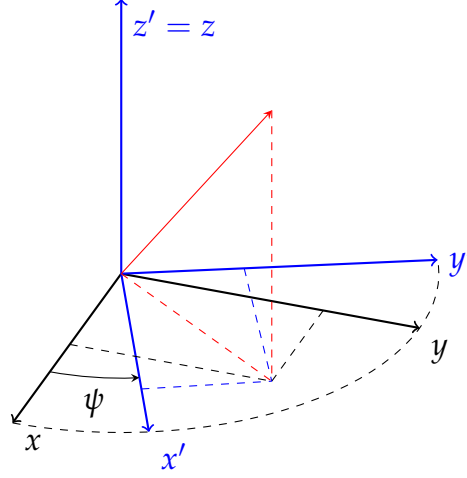
Figure 3.2: An exemplary coordinate rotation about the *z*-axis by an angle ψ, illustrating the orthogonal projection on the resulting axes x', y', z'.

Note that $\mathbf{C}_{bn} = \mathbf{C}_{nb}^{T} = \mathbf{C}_{nb}^{-1}$, so that $\mathbf{C}_{bn}\mathbf{C}_{nb} = \mathbf{I}$.

3.3 Quaternions

Quaternions are a number system that extends the complex numbers. They were first described by Irish mathematician William Rowan Hamilton in 1843. The set of quaternions is equal to $\mathbb{R}^4$ and denoted $\mathbb{H}$. A quaternion $\mathbf{q} \in \mathbb{H}$ may be represented as a vector

$$\mathbf{q} = q_0 + q_1 i + q_2 j + q_3 k = \begin{bmatrix} q_0, & q_1, & q_2, & q_3 \end{bmatrix}^T = \begin{bmatrix} q_0 \\ \mathbf{q}_{1:3} \end{bmatrix}, \qquad (3.4)$$

whereby the following relations between the imaginary units i, j, k hold:

$$i^2 = j^2 = k^2 = ijk = -1,$$

$$\begin{aligned} ij &= k, & ji &= -k, \\ jk &= i, & kj &= -i, \\ ki &= j, & ik &= -j. \end{aligned} \qquad (3.5)$$

The *adjoint*, *norm* and *inverse* of a quaternion are defined as

$$\bar{\mathbf{q}} = \begin{bmatrix} q_0 \\ -\mathbf{q}_{1:3} \end{bmatrix}, \qquad (3.6)$$

$$||\mathbf{q}|| = \sqrt{q_0^2 + q_1^2 + q_2^2 + q_3^2} \tag{3.7}$$

$$\mathbf{q}^{-1} = \frac{\bar{\mathbf{q}}}{||\mathbf{q}||} \tag{3.8}$$

The sum of two quaternions is defined as

$$\mathbf{q} + \mathbf{p} = \begin{bmatrix} q_0 + p_0 \\ \mathbf{q}_{1:3} + \mathbf{p}_{1:3} \end{bmatrix}. \tag{3.9}$$

Quaternion multiplication is defined as

$$\mathbf{qp} = \begin{bmatrix} q_0 p_0 - \mathbf{q}_{1:3}^T \mathbf{p}_{1:3} \\ q_0 \mathbf{p}_{1:3} + p_0 \mathbf{q}_{1:3} - \mathbf{q}_{1:3} \times \mathbf{p}_{1:3} \end{bmatrix}, \tag{3.10}$$

and can be written as the second quaternion left-multiplied by a matrix-valued function Q of the first quaternion.

$$\mathbf{qp} = Q(\mathbf{q})\mathbf{p} = \bar{Q}(\mathbf{p})\mathbf{q} \tag{3.11}$$

The *quaternion matrix function*, $Q : \mathbb{H} \rightarrow \mathbb{R}^{4 \times 4}$ is defined by

$$Q(\mathbf{q}) = \begin{bmatrix} q_0 & -q_1 & -q_2 & -q_3 \\ q_1 & q_0 & q_3 & -q_2 \\ q_2 & -q_3 & q_0 & q_1 \\ q_3 & q_2 & -q_1 & q_0 \end{bmatrix}, \tag{3.12}$$

and the *conjugate quaternion matrix function*, $\bar{Q} : \mathbb{H} \rightarrow \mathbb{R}^{4 \times 4}$ is defined by

$$\bar{Q}(\mathbf{q}) = \begin{bmatrix} q_0 & -q_1 & -q_2 & -q_3 \\ q_1 & q_0 & -q_3 & q_2 \\ q_2 & q_3 & q_0 & -q_1 \\ q_3 & -q_2 & q_1 & q_0 \end{bmatrix}. \tag{3.13}$$

Unit quaternions, that is quaternions with unity norm, can be used to represent rotations in three dimensional space. Let $z \in \mathbb{R}^3$ be an arbitrary vector in the navigation frame and let $z' \in \mathbb{R}^3$ be the same vector in the body frame. Furthermore, let $\mathbf{r}$ be a quaternion with $||\mathbf{r}|| = 1$. Then the following relations hold:

$$\begin{bmatrix} 0 \\ \mathbf{z}' \end{bmatrix} = \mathbf{r} \begin{bmatrix} 0 \\ \mathbf{z} \end{bmatrix} \mathbf{r}^{-1}, \tag{3.14}$$

$$\begin{bmatrix} 0 \\ \mathbf{z} \end{bmatrix} = \mathbf{r}^{-1} \begin{bmatrix} 0 \\ \mathbf{z'} \end{bmatrix} \mathbf{r}. \tag{3.15}$$

Sequences of rotations can thus be represented by products of quaternions. The quaternion for a single rotation by α about the axis $\boldsymbol{\epsilon} \in \mathbb{R}^3$, $||\boldsymbol{\epsilon}|| = 1$, is given by

$$\mathbf{r}_{\epsilon}(\alpha) = \begin{bmatrix} \cos\frac{\alpha}{2}, & \boldsymbol{\epsilon}\sin\frac{\alpha}{2} \end{bmatrix}^T = \begin{bmatrix} \cos\frac{\alpha}{2}, & \epsilon_1\sin\frac{\alpha}{2}, & \epsilon_2\sin\frac{\alpha}{2}, & \epsilon_3\sin\frac{\alpha}{2} \end{bmatrix}^T. \tag{3.16}$$

The reverse mapping from quaternions to Euler angles is given by

$$\begin{bmatrix} \phi \\ \theta \\ \psi \end{bmatrix} = \begin{bmatrix} \mathrm{atan2}(\frac{(2(q_0q_1+q_2q_3)}{1-2(q_1^2+q_2^2)}) \\ \arcsin(2(q_0q_2-q_3q_1)) \\ \mathrm{atan2}(\frac{2(q_0q_3+q_1q_2)}{1-2(q_2^2+q_3^2)}) \end{bmatrix}. \tag{3.17}$$

Quaternions are less intuitive than Euler angles. Nevertheless, they are very popular in attitude representation, since they are mathematically elegant and don't suffer from singularities.

3.4 Projection of Gravity Vector and Earth's Magnetic Field Vector

As described in Chapter 2, accelerometers measure the acceleration they experience. Under static or quasi-static (steady, linear motion) conditions, or at low acceleration it can be assumed that the measured acceleration is mainly that of gravity. Be means of simple trigonometric transformations estimates for the pitch and the roll angle can be obtained. Since the gravity vector is perpendicular to the *xy*-plane and thus a rotation around the *z*-axis will not cause any variation in the sensed acceleration, the yaw angle cannot be obtained by this method. To solve this problem a three-dimensional magnetometer is used, which measures the variation of Earth's magnetic field while rotating around the *z*-axis.

When the accelerometer is motionless, its measurements will be directly related to the angle of the sensor relative to gravity, as depicted in Figure 3.3 (a). In that case θ is given by

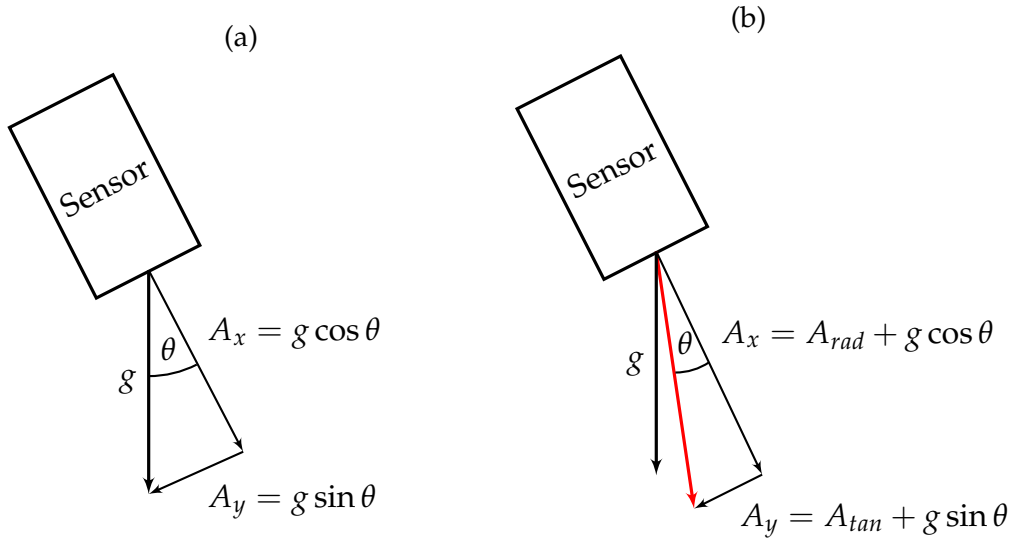$$\theta = \mathrm{atan2}(\frac{A_y}{A_x}). \tag{3.18}$$

Figure 3.3: Acceleration seen by the sensor (b) with and (a) without motion from [4].

However, when the sensor is in motion, in addition to the gravity, there are radial and tangential acceleration components due to motion, as depicted in Figure 3.3 (b). Ignoring these components will cause incorrect angle estimates.

3.5 Integration of Angular Rate

Another way to estimate the attitude of an object is the integration of the angular rate around the x, y and z-axis, respectively. Although this would theoretically lead to very accurate orientation estimates, they are impaired by angle random walk (ARW) and dynamical bias in practice. ARW is an effect caused by the integration of high-frequency, thermo-mechanical noise, which leads to a random additive angle in the orientation signal. An even greater impact than AWR has the gyroscopes dynamic bias, which has its origin in low-frequency flicker noise. Both effects cause a dramatical drift in the angle signal over time.

Quaternions are very well suited to tracking the attitude of an object by integrating the body-fixed angular velocity over time...

3.6   Sensor Fusion

Since the projection of the gravity vector and the Earth's magnetic field vector are only valid under static or quasi-static conditions, or at low acceleration, and the integration of the angular rate leads to non-reliable estimates due to suffering from ARW and dynamic bias, but is not affected by the intensity of motion, a means to combine the information of both sensors is desirable. The combination of information from multiple sensors to increase the overall precision of the estimation of a certain quantity of interest is termed sensor fusion. Raol [27] states the following advantages of sensor fusion:

- Robust functional and operational performance is given, in case of data loss from one sensor, due to redundancy provided by multiple sensors.

- Enhanced confidence in the results inferred from the measurement of one sensor, if they are confirmed by the measurement of another sensor.

- With sensor fusion an arbitrary fine time resolution of measurements is possible, whereas single sensors need a finite time to transmit measurements and so limit the frequency of measurements.

- One sensor might be, to some extent, better in a certain state of the measured process, e.g. low or high motion intensity in attitude estimation, and thus, by fusing multiple sensor signals, a satisfactory accuracy among all states of the process could be attained.

Sensor fusion can be realised by the use of a Kalman filter, which is described in detail in the next chapter.

Chapter 4

Digital Filters

Conceived in general terms, a filter is a physical device for removing unwanted components of a mixture. In the technical field a filter is a system designed to extract information from noisy measurements of a process. That is, the filter delivers an estimate of the variables of principal interest, which is why it may also be called an estimator. Filter theory is applied in diverse fields of science and technology, such as communications, radar, sonar, navigation, and biomedical engineering [5].

In contrast to analogue filters that consist of electronic circuits to attenuate unwanted frequencies in continuous-time signals and thus extracted the useful signal, a digital filter is a set of mathematical operations applied to a discrete-time signal in order to extract information about the hidden quantity of interest. A discrete-time signal is a sequence of samples at equidistant time instants that represent the continuous-time signal with no loss, provided the sampling theorem is satisfied, according to which the sample frequency has to be greater than twice the highest frequency component of the continuous-time signal.

Digital filters can be classified as linear and nonlinear. If the quantity at the output of the filter is a linear function of its input, that is, the filter function satisfies the superposition principle, the filter is said to be linear. Otherwise, the filter is nonlinear.

4.1 The Filtering Problem

Consider, as an example involving filter theory, the continuous-time dynamical system depicted in Figure 4.1. The desired state vector of the
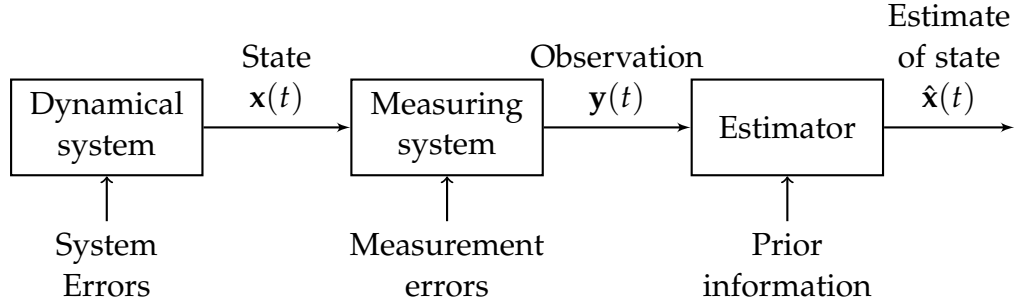
Figure 4.1: Block diagram depicting the components involved in state estimation from [5].

system, $\mathbf{x}(t)$, is usually hidden and can only be observed by indirect measurements $\mathbf{y}(t)$ that are a function of $\mathbf{x}(t)$ and subject to noise. Equally, the equation describing the evolution of the state $\mathbf{x}(t)$ is usually subject to system errors. These could be caused by, for instance, effects not accounted for in the model. The dynamical system may be an aircraft in flight, in which case the elements of the state vector are constituted by its position and velocity. The measuring system may be a tracking radar producing the observation vector $\mathbf{y}(t)$ over an interval $[0, T]$. The requirement of the filter is to deliver a reliable estimate $\hat{\mathbf{x}}(t)$ of the actual state $\mathbf{x}(t)$, by taking the measurement as well as prior information into account.

4.2   Wiener Filters

A statistical criterion, according to which the performance of a filter can be measured, is the mean-squared error. Consider the linear dicrete-time filter with the impulse response $w_0, w_1, w_2, \ldots$ depicted in Figure 4.2. At some discrete time n it produces an output designated by $\hat{x}(n)$, which provides an estimate of a desired response denoted by $d(n)$. According to Haykin [5] the essence of the filtering problem and the resulting requirement is summarised with the following statement:

> "Design a linear discrete-time filter whose output $\hat{x}(n)$ provides an estimate of the desired response $d(n)$, given a set of input samples $y(0), y(1), y(2), \ldots$, such that the mean-square value of the estimation error $e(n)$, defined as the difference between the desired response $d(n)$ and the actual response $\hat{x}(n)$, is minimized."
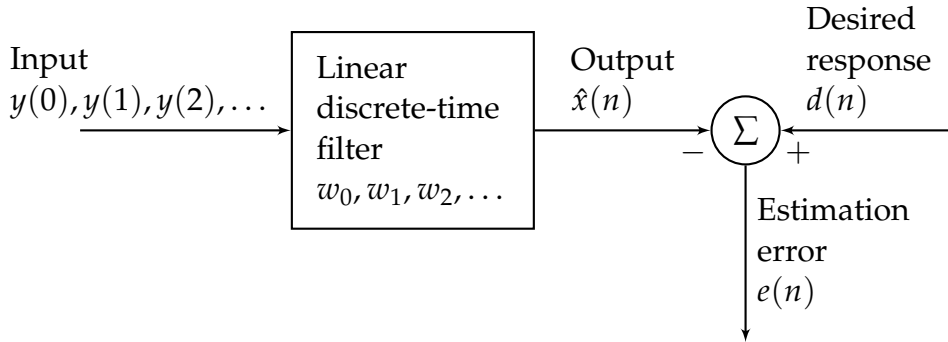
Figure 4.2: Block diagram representation of the statistical filtering problem from [5].

Assume a stationary stochastic process with known statistical parameters as the mean and correlation functions of the useful signal and the unwanted additive noise. Then, the solution to this statistical optimisation problem is commonly known as the Wiener filter. Yet, since the Wiener filter requires a priori information about the statistics of the data to be processed, it may not be optimum for non-stationary processes. For such an environment, in which the statistics are time-vaying, it needs a filter that constantly adapts its parameters to optimise its output.

4.3   Adaptive Filters

A possible approach to mitigate the limitations of the Wiener filter for non-stationary processes is the 'estimate and plug' procedure. The filter 'estimates' the statistical parameters of the relevant signals and 'plugs' them into a non-recursive formula for computing the filter parameters. This procedure requires excessively elaborate and costly hardware for real-time operation [5]. To overcome this disadvantage one may use an adaptive filter, which is a self-designing system that relies, in contrast, on a recursive algorithm. It allows the filter to perform satisfactorily even if there is no complete knowledge of the relevant signal characteristics. Provided the variations in the statistics of the input data are sufficiently slow, the algorithm can track time variations and is thus suitable for non-stationary environments. The algorithm starts from some predetermined set of initial conditions respecting the knowledge about the system. In a stationary environment it converges to the optimum Wiener solution in

some statistical sense after successive iterations. The Kalman filter is such an adaptive filter.

Due to the fact that the parameters of an adaptive filter are updated each iteration, they become data dependent. The system does not obey the principles of superposition which therefore makes the adaptive filter in reality a nonlinear system. However, an adaptive filter is commonly said to be linear if its input-output map satisfies the superposition principle, as long as its parameters are held fixed. Otherwise it is said to be nonlinear.

4.4   The Kalman Filter

The Kalman filter is a set of recursive mathematical equations that provides an efficient means to estimate the state of a linear dynamic system perturbed by additive white Gaussian noise, even when the precise nature of the modelled system is unknown. It incorporates knowledge of the system and measurement device dynamics, the statistical description of the system errors and measurement noise, uncertainty in the dynamics model, and available information about initial conditions of the variables of interest, to produce an estimate of these variables, in a way that the mean of the squarred error is minimised [6].

The filter is named after Rudolf E. Kalman who 1960 published his famous paper describing a recursive solution to the discrete-data linear filtering problem [28]. Since that time, the Kalman filter has been the subject of extensive research, due, to a large extent, to the advances in digital computing [29]. It finds applications in autonomous and assisted navigation, more examples missing, among others.

The following introductory example from [6] is an illustrative description of the determination of a one-dimensional position to understand how the Kalman filter works.

4.4.1   An Introductory Example

Suppose you are lost at sea during the night and take a star sighting to determine your approximate position at time t_1 to be z_1. Your location estimate is, due to inherent measurement device inaccuracies and human error, somewhat uncertain, and thus assumed to be associated with a standard deviation σ_{z_1}. The conditional probability of $x(t_1)$, your actual
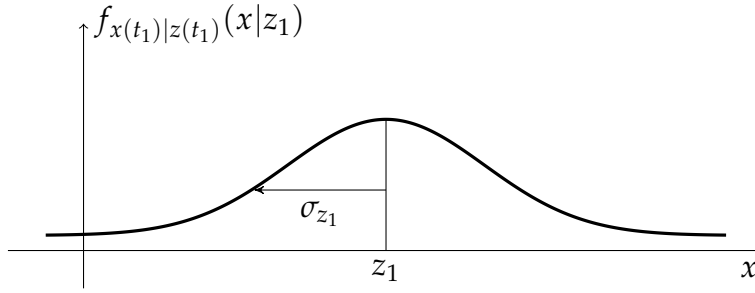
Figure 4.3: Conditional density of position based on measurement value z_1 from [6].

position at time t_1, conditioned on the observed value z_1, is depicted in Figure 4.3. The best estimate of your position, based on this conditional probability density, is

$$\hat{x}(t_1) = z_1 \tag{4.1}$$

and the variance of the error in the estimate is

$$\sigma_x^2(t_1) = \sigma_{z_1}^2 . \tag{4.2}$$

Right after you, say a trained navigator friend takes an independent fix at time $t_2 \cong t_1$, so that the true position has not changes at all. He obtains a measurement z_2 with a variance σ_{z_2}, which is somewhat smaller than yours, since he has a higher skill. Figure 4.4 depicts the conditional density of your position at time t_2, based only on the measurement value z_2. Combining these data, your position at time $t_2 \cong t_1$, $x(t_2)$, given both z_1 and z_2, is then a Gaussian density with mean μ and variance σ^2, as indicated in Figure 4.5, with

$$\mu = z_1 \frac{\sigma_{z_2}^2}{\sigma_{z_1}^2 + \sigma_{z_2}^2} + z_2 \frac{\sigma_{z_1}^2}{\sigma_{z_1}^2 + \sigma_{z_2}^2} \tag{4.3}$$

and

$$\frac{1}{\sigma^2} = \frac{1}{\sigma_{z_1}^2} + \frac{1}{\sigma_{z_2}^2} . \tag{4.4}$$

The uncertainty in your estimate of position has been decreased because σ is less than either $\sigma_{z_1}^2$ or $\sigma_{z_2}^2$. Even if σ_{z_1} was very large, the variance of the estimate is less than σ_{z_2}, which means that even poor quality data
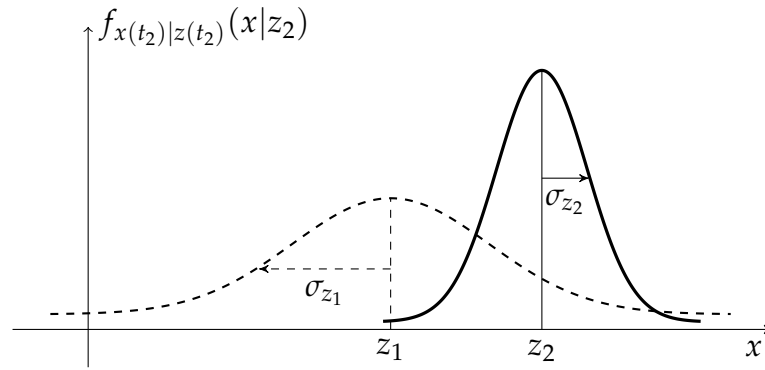
Figure 4.4: Conditional density of position based on measurement value z_2 alone from [6].
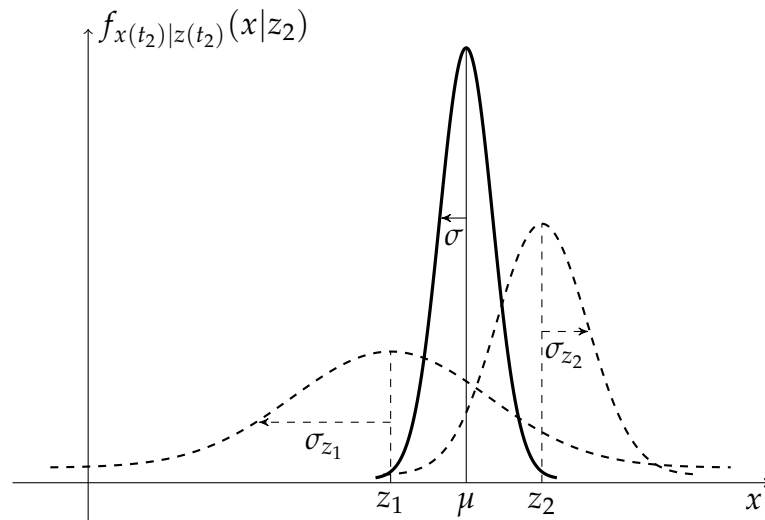

Figure 4.5: Conditional density of position based on data z_1 and z_2 from [6].

increases the precision of the filter output. The best estimate, given this density, is

$$\hat{x}(t_2) = \mu, \tag{4.5}$$

with an associated error variance σ^2.

Having a closer look at the form of μ in Equation 4.3, one notices that it makes good sense. If the measurements were of equal precision, meaning $\sigma_{z_1} = \sigma_{z_2}$, the optimal estate is simply the average of both measurements, as would be expected. If σ_{z_1} is larger than σ_{z_2}, the equation weights z_2 more heavily than z_1.

Equation 4.5 for the filter output can be written as

$$
\begin{aligned}
\hat{x}(t_2) &= z_1 \frac{\sigma_{z_2}^2}{\sigma_{z_1}^2 + \sigma_{z_2}^2} + z_2 \frac{\sigma_{z_1}^2}{\sigma_{z_1}^2 + \sigma_{z_2}^2} \\
&= z_1 + \frac{\sigma_{z_1}^2}{\sigma_{z_1}^2 + \sigma_{z_2}^2} [z_2 - z_1]
\end{aligned}
\tag{4.6}
$$

or in a form that is used in Kalman filter implementations, with $\hat{x}(t_1) = z_1$, as

$$\hat{x}(t_2) = \hat{x}(t_1) + K(t_2)[z_2 - \hat{x}(t_1)], \tag{4.7}$$

where

$$K(t_2) = \frac{\sigma_{z_1}^2}{\sigma_{z_1}^2 + \sigma_{z_2}^2}. \tag{4.8}$$

These equation represent the 'predictor-corrector' structure of the Kalman filter. A prediction of the value that the desired variables and the measurements will have at the next measurement time is made, based on all previous information. Then the difference between the measurement and its predicted value is used to correct the prediction of the desired variables. According to Equation 4.7 the optimal estimate at time t_2, $\hat{x}(t_2)$, is equal to $\hat{x}(t_1)$, the best prediction of its value before z_2 is taken, plus a correction term of an optimal weighting value times the difference between z_2 and the best prediction of it before the measurement is actually taken.

To incorporate dynamics into the model, suppose you travel for some time before taking another measurement. The best model you have for your motion may be of the form
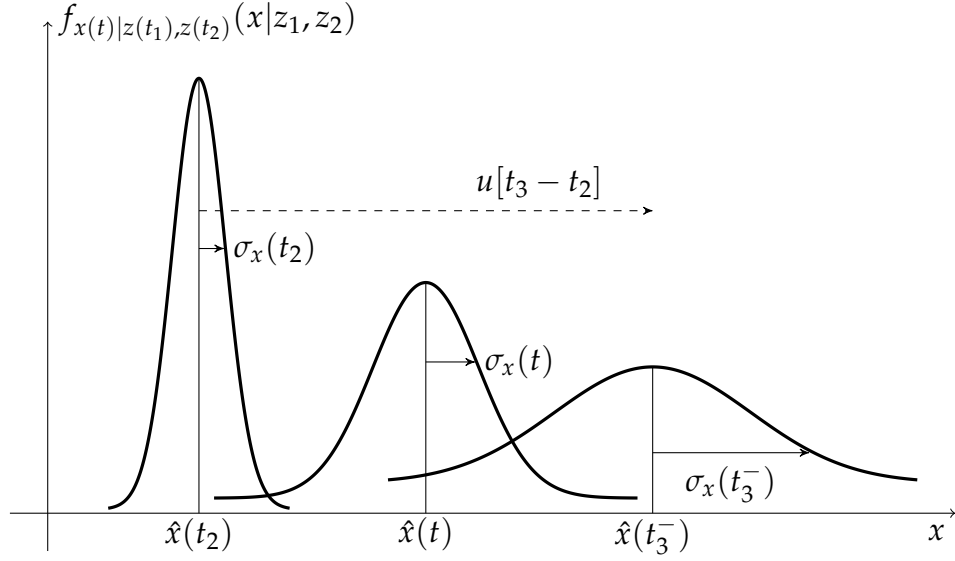
Figure 4.6: Propagation of conditional probability density from [6].

$$\frac{dx}{dt} = u + w, \tag{4.9}$$

where u is a nominal velocity and w is a noise term, representing the uncertainty in your knowledge of the actual velocity due to disturbances and effects not accounted for in the simple first order equation. It will be modeled as white Gaussian noise with a mean of zero and variance of σ_w^2.

The conditional density of the position at time t_2, given z_1 and z_2, was previously derived. Figure 4.6 shows graphically how the density travels along the x-axis as time progresses. It start at the best estimate and moves according to the above mentioned model of dynamics. Due to the constant addition of uncertainty over time it spreads out. As the variance becomes greater you become less sure of your position. The Gaussian density $f_{x(t_3)|z(t_1),z(t_2)}(x|z_1,z_2)$ can be expressed mathematically by its mean and variance given by

$$\hat{x}(t_3^-) = \hat{x}(t_2) + u[t_3 - t_2] \tag{4.10}$$

$$\sigma_x^2(t_3^-) = \sigma_x^2(t_2) + \sigma_w^2[t_3 - t_2] \tag{4.11}$$

$\hat{x}(t_3^-)$ is the optimal prediction of the location at t_3^- before the measurement is taken at t_3, associated with the variance in this prediction, $\sigma_x^2(t_3^-)$.

Now a measurement z_3 with an assumed variance $\sigma_{z_3}^2$ is taken. As before, its conditional probability density is combined with the density with mean $\hat{x}(t_3^-)$ and variance $\sigma_x^2(t_3^-)$, to yield a Gaussian density with mean

$$\hat{x}(t_3) = \hat{x}(t_3^-) + K(t_3)[z_3 - \hat{x}(t_3^-)] \tag{4.12}$$

and variance

$$\sigma_x^2(t_3) = \sigma_x^2(t_3^-) - K(t_3)\sigma_x^2(t_3^-), \tag{4.13}$$

where the gain $K(t_3)$ is given by

$$K(t_3) = \frac{\sigma_x^2(t_3^-)}{\sigma_x^2(t_3^-) + \sigma_{z_3}^2}. \tag{4.14}$$

Observing the form of Equation 4.14 the reasonableness of the filter structure becomes obvious. If the variance of the measurement noise $\sigma_{z_3}^2$ is large, then $K(t_3)$ is small, meaning that little confidence is put in a very noisy measurement and that it is weighted lightly. For $\sigma_{z_3}^2 \to \infty$, $K(t_3)$ becomes zero, and $\hat{x}(t_3)$ equals $\hat{x}(t_3^-)$. Thus, an infinitely noisy measurement is totally ignored. Likewise, if the dynamical system noise variance σ_w^2 is large, then according to Equation 4.11, $\sigma_x^2(t_3^-)$ will be large, and so will be $K(t_3)$. Therefore, the measurement is weighted heavily, in case you are not very certain about the output of the system model within the filter structure. In the limit as $\sigma_w^2 \to \infty$, $\sigma_x^2(t_3^-) \to \infty$, and $K(t_3) \to 1$, so Equation 4.5 yields

$$\hat{x}(t_3) = \hat{x}(t_3^-) + 1 \cdot [z_3 - \hat{x}(t_3^-)] = z_3. \tag{4.15}$$

That means that in the limit of absolutely no confidence in the system model output, solely the new measurement is taken as the optimal estimate. Finally, if you are absolutely sure of your estimate before z_3 comes available, $\sigma_x^2(t_3^-)$ would become zero, and so would $K(t_3)$, which means that the measurements would be left disregarded.

Extending Equations 4.10, 4.11, 4.12 and 4.14 to the vector case and allowing time varying parameters in the system and noise description leads to the general Kalman filter equations.

4.4.2 Formulation of the Kalman Filter Equations

Let $\mathbf{x}_k \in \mathbb{R}^n$ be the state vector of a discrete-time controlled process governed by the linear stochastic difference equation

$$\mathbf{x}_k = \mathbf{\Phi}_{k-1}\mathbf{x}_{k-1} + \mathbf{B}_{k-1}\mathbf{u}_{k-1} + \mathbf{w}_{k-1} \tag{4.16}$$

and $\mathbf{z}_k \in \mathbb{R}^m$ the observation or measurement vector of this process, given by

$$\mathbf{z}_k = \mathbf{H}_k\mathbf{x}_k + \mathbf{v}_k \,, \tag{4.17}$$

where the index $k \in \mathbb{N}^0$ denotes discrete time normalised to the sampling interval. The $n \times 1$ vector w_k and the $m \times 1$ vector v_k represent the process noise and the measurement noise, respectively, modelled as zero-mean, Gaussian white noise

$$\mathbf{w}_k \sim \mathcal{N}(0, \mathbf{Q}_k) \,, \tag{4.18}$$

$$\mathbf{v}_k \sim \mathcal{N}(0, \mathbf{R}_k) \,, \tag{4.19}$$

with the the process noise covariance matrix $\mathbf{Q}_k$ and the measurement noise covariance matrix $\mathbf{R}_k$. They are assumed to be uncorrelated. The $n \times n$ transition matrix $\mathbf{\Phi}_k$ in 4.16 relates the state at the previous time step $k-1$ to the state at the current step k. The $n \times l$ matrix $\mathbf{B}_k$ relates the optional control input $\mathbf{u}_k \in \mathbb{R}^l$ to the state $\mathbf{x}_k$. Finally, the $m \times n$ measurement matrix $\mathbf{H}_k$ in 4.17 relates the state $\mathbf{x}_k$ to the measurement $\mathbf{z}_k$.

The Kalman filter solves the problem of estimating the state $\mathbf{x}_k$ of the given linear stochastic system, represented by $\hat{\mathbf{x}}_k$, which is also a linear function of the measurement $\mathbf{z}_k$, minimising the weighted mean-squarred error. This problem is called the *linear quadratic Gaussian* estimation problem; the dynamic system is linear, the performance cost function is quadratic, and the random process is Gaussian.

We define the vector $\hat{\mathbf{x}}_k^- \in \mathbb{R}^n$ as the *a priori* state estimate representing knowledge of the process prior to step k and $\hat{\mathbf{x}}_k \in \mathbb{R}^n$ as the *a posteriori* state estimate at step k given the measurement $\mathbf{z}_k$:

$$\hat{\mathbf{x}}_k^- = \mathbf{\Phi}_{k-1}\hat{\mathbf{x}}_{k-1} + \mathbf{B}_{k-1}\mathbf{u}_{k-1} \,, \tag{4.20}$$

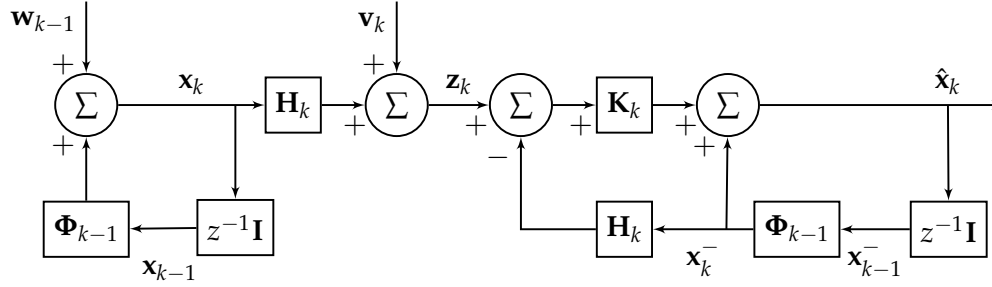$$\hat{\mathbf{x}}_k = \hat{\mathbf{x}}_k^- + \mathbf{K}_k[\mathbf{z}_k - \mathbf{H}_k\hat{\mathbf{x}}_k^-] \,. \tag{4.21}$$

Figure 4.7: Block diagram depicting the relation between a discrete-time dynamical system, its observation, and the Kalman filter.

The term $[\mathbf{z}_k - \mathbf{H}_k\hat{\mathbf{x}}_k^-]$ is called the measurement innovation or residual. It reflects the discordance between the predicted measurement $\mathbf{H}_k\hat{\mathbf{x}}_k^-$ and the actual measurement $\mathbf{z}_k$. The $n \times m$ matrix $\mathbf{K}_k$ is termed the Kalman gain and is given by

$$\mathbf{K}_k = \mathbf{P}_k^- \mathbf{H}_k^T [\mathbf{H}_k \mathbf{P}_k^- \mathbf{H}_k^T + \mathbf{R}_k]^{-1}, \tag{4.22}$$

with

$$\mathbf{P}_k^- = \boldsymbol{\Phi}_{k-1} \mathbf{P}_{k-1} \boldsymbol{\Phi}_{k-1}^T + \mathbf{Q}_{k-1} \tag{4.23}$$

and

$$\mathbf{P}_k = [\mathbf{I} - \mathbf{K}_k \mathbf{H}_k] \mathbf{P}_k^- . \tag{4.24}$$

Figure 4.7 illustrates the relation of the Kalman filter to the discrete-time dynamical system, where z^{-1} denotes the unit-delay and $\mathbf{I}$ the $n \times n$ identity matrix.

The Kalman filter equations can be divided into two groups: *time update* Equations 4.20, 4.23 and *measurement update* Equations 4.21 , 4.22, and 4.24, as seen in Figure 4.9, which shows the predict and update behaviour of the filter algorithm.

4.5   The Extended Kalman Filter

Up to this point the Kalman filter has solved the filtering problem for linear time-dynamical systems. One may extend the Kalman filter to systems with state dynamics governed by non-linear state transformations
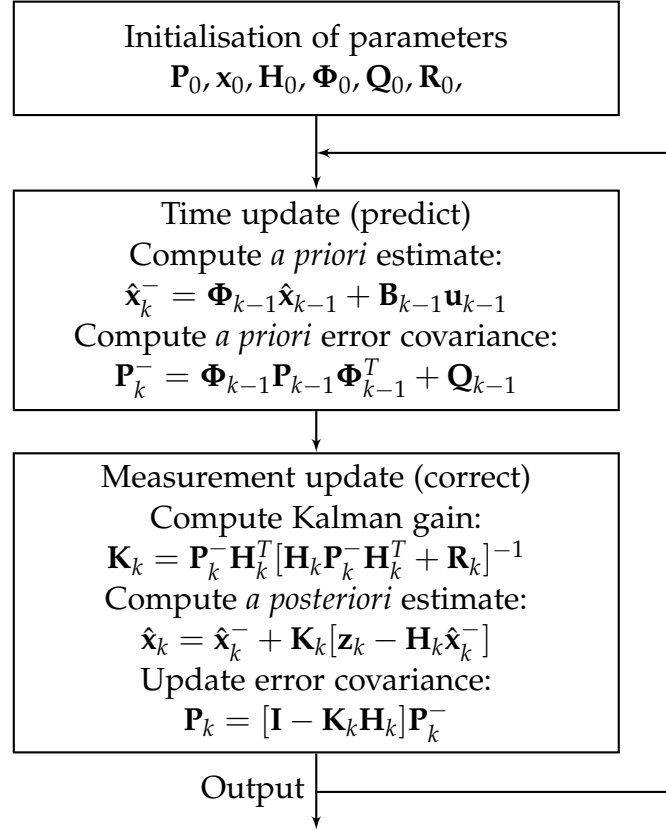
Figure 4.8: Operation cycle of the Kalman filter algorithm illustrating predict and correct behaviour.

$$\mathbf{x}_k = \boldsymbol{\phi}_{k-1}(\mathbf{x}_{k-1}) + \mathbf{w}_{k-1}, \quad \mathbf{w}_k \sim \mathcal{N}(0, \mathbf{Q}_k), \tag{4.25}$$

and/or with a non-linear transformation from state variables to measurement variables

$$\mathbf{z}_k = \mathbf{h}_k(\mathbf{x}_k) + \mathbf{v}_k, \quad \mathbf{v}_k \sim \mathcal{N}(0, \mathbf{R}_k). \tag{4.26}$$

The *functional* $\boldsymbol{\phi}_{k-1}$ denotes the *non-linear* transition matrix function that may be time varying. It relates the state at the previous time step $k-1$ to the current time step k. The functional $\mathbf{h}_k$ denotes a *non-linear* measurement matrix function that relates the state $\mathbf{x}_k$ to the measurement $\mathbf{z}_k$ and is possibly time varying, too.

Some non-linear problems can be deemed *quasilinear*, which means that the variation of the non-linear functionals $\boldsymbol{\phi}$ and $\mathbf{h}$ are predominantly linear about the value $\mathbf{x}$. That is,

$$\boldsymbol{\phi}_k(\mathbf{x} + d\mathbf{x}) \approx \boldsymbol{\phi}_k(\mathbf{x}) + d\mathbf{x} \left. \frac{\partial \boldsymbol{\phi}_k(\mathbf{x})}{\partial \mathbf{x}} \right|_{\mathbf{x}}, \tag{4.27}$$

$$\mathbf{h}_k(\mathbf{x} + d\mathbf{x}) \approx \mathbf{h}_k(\mathbf{x}) + d\mathbf{x} \left. \frac{\partial \mathbf{h}_k(\mathbf{x})}{\partial \mathbf{x}} \right|_{\mathbf{x}}, \tag{4.28}$$

which requires that $\boldsymbol{\phi}$ and $\mathbf{h}$ are differentiable at $\mathbf{x}$.

Through a *linearisation* of the state-space model of Equations 4.25 and 4.26 at each time instant around the most recent state estimate, the standard Kalman filter equation from Section 4.4.2 can be applied. The filter resulting from a *linear approximation* of the state transitions and the relation of the measurement to the respective state is referred to as the *extended Kalman filter* (EKF).

The Jacobian matrices of the functionals $\boldsymbol{\phi}$ and $\mathbf{h}$, which are employed in the linearisation, are given by

$$\boldsymbol{\Phi}_{k-1}^{[1]} = \left. \frac{\partial \boldsymbol{\phi}_{k-1}(\mathbf{x})}{\partial \mathbf{x}} \right|_{\mathbf{x} = \hat{\mathbf{x}}_{k-1}^-}, \tag{4.29}$$

and

$$\mathbf{H}_k^{[1]} = \left. \frac{\partial \mathbf{h}_k(\mathbf{x})}{\partial \mathbf{x}} \right|_{\mathbf{x} = \hat{\mathbf{x}}_k^-}. \tag{4.30}$$

The ij^{th} entry of $\boldsymbol{\Phi}_{k-1}^{[1]}$ is equal to the partial derivative of the ith component of $\boldsymbol{\phi}_{k-1}(\mathbf{x})$ with respect to the jth component of $\mathbf{x}$. The derivatives are evaluated at $\mathbf{x} = \hat{\mathbf{x}}_{k-1}^-$. Likewise, the ij^{th} entry of $\mathbf{H}_{k-1}^{[1]}$ is equal to the partial derivative of the ith component of $\mathbf{h}_k(\mathbf{x})$ with respect to the jth component of $\mathbf{x}$. The derivatives are evaluated at $\mathbf{x} = \hat{\mathbf{x}}_k^-$. The superscript $[1]$ denotes the first-order approximation.

The predicted state estimate is given by

$$\hat{\mathbf{x}}_k^- = \boldsymbol{\phi}_{k-1}(\mathbf{x}_{k-1}), \tag{4.31}$$

and the predicted measurement by

$$\hat{\mathbf{z}}_k = \mathbf{h}_k(\mathbf{x}_k^-). \tag{4.32}$$

The *a posteriori* estimate is then, conditioned on the actual measurement,

$$\hat{\mathbf{x}}_k = \hat{\mathbf{x}}_k^- + \mathbf{K}_k[\mathbf{z}_k - \hat{\mathbf{z}}_k]. \tag{4.33}$$

The a priori covariance matrix $\mathbf{P}_k^-$, the cooresponding Kalman gain $\mathbf{K}_k$, and the a posteriori covariance matrix $\mathbf{P}_k$ are equal to Equations 4.35, 4.23, and 4.24 in Section 4.4.2 but reproduced here for convenience of presentation:

$$\mathbf{P}_k^- = \mathbf{\Phi}_{k-1}^{[1]} \mathbf{P}_{k-1} \mathbf{\Phi}_{k-1}^{[1]T} + \mathbf{Q}_{k-1} \tag{4.34}$$

$$\mathbf{K}_k = \mathbf{P}_k^- \mathbf{H}_k^{[1]T} [\mathbf{H}_k^{[1]} \mathbf{P}_k^- \mathbf{H}_k^{[1]T} + \mathbf{R}_k]^{-1} \tag{4.35}$$

$$\mathbf{P}_k = [\mathbf{I} - \mathbf{K}_k \mathbf{H}_k^{[1]}] \mathbf{P}_k^- \tag{4.36}$$

Figure 4.9 illustrates the predict and update behaviour of the extended Kalman filter algorithm.
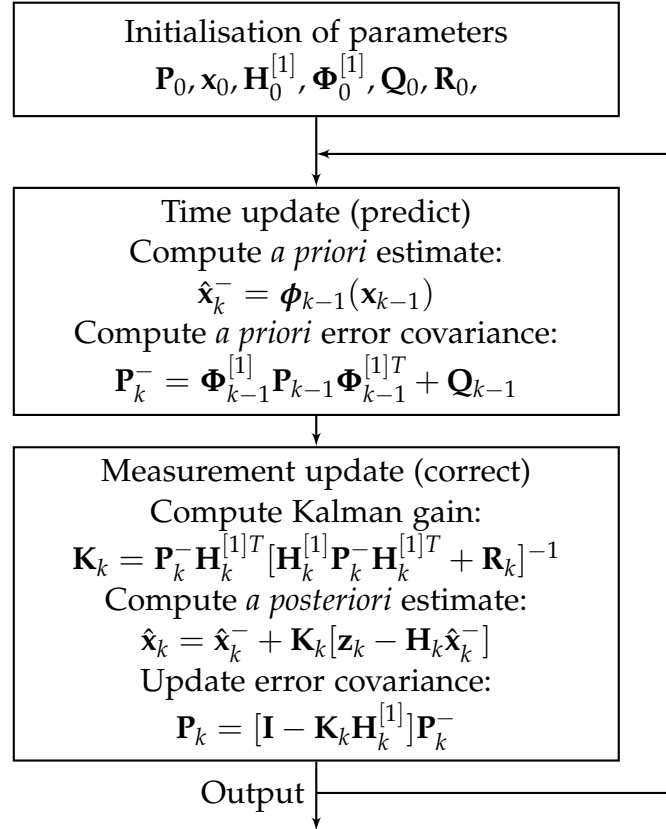

Figure 4.9: Operation cycle of the extended Kalman filter algorithm illustrating predict and correct behaviour.

Chapter 5

Implementation

This chapter describes the theoretical design of the system and the implementation, based on the fundamentals acquired in the previous the chapters. Subsequently, the experiments and its results are presented.

5.1 Initial Situation

(Any algorithms that are already implemented for comparison that I can cite or state and describe how they differ from the one that I will implement??)

5.2 Theoretical Design

According to Bennett et al. [4], when walking in a straight line, the human leg can be modelled as a two-link planar revolute robot. As depicted in Figure 5.1, the revolute joints represent the hip und knee joint, and the two links the thigh and shank, respectively.

5.3 Implementation

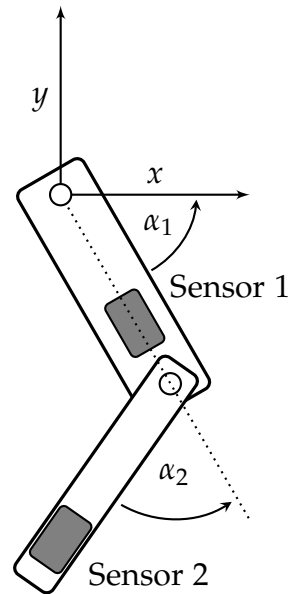The filter algorithm was implemented in MATLAB®.

Figure 5.1: Acceleration seen by the sensor (b) with and (a) without motion from [4].

5.4   Experiments

5.5   Results

5.6   Discussion

Chapter 6

Conclusion and Future Work

6.1 Conclusions

Summarising the above, I can say that I have learned a lot in the four month that I spent in Granada. Amongst others I have come to know many new work methods, not only due to being exposed to people from a different culture, but also due to the fact that scientific research differs strongly from the work as a student at university. I gained a deeper understanding of orientation estimation and how Kalman filtering improves those. Therefore I had to study the principles of Kalman filters as well as the basics of MARG sensors. I was able to improve my MATLAB® skills and have realised how important it is to write understandable and well commented code, if it is for a larger project and not only for a coursework. I am now familiar with tools such as GitHub and Pivotal Tracker which make working in a team much easier and significantly more efficient. Beside my work at the research centre, where I obtained a valuable insight into scientific research, I read a book about scientific writing that helped me to improve my oral and written English skills during my stay. Furthermore I now know the fundamentals of LaTeX.

All in all it was a great experience, professionally as well as personally. I truly and unreservedly recommend such a stay to every university student.

6.2   Future Work

Biomedical research is a very interesting blend of both my major interests, that is, working in the medical field as a paramedic and in the technical field as an electrical engineer. There is a variety of possible future work. One related topic would be the validation of the pitch angles measured with the gyroscopes of the GaitWatch by means of cameras that record the trace of visual markers. From these markers one could compute the pitch angels and compare them to the those of the GaitWatch.

Bibliography

[1] Jussi Collin, Pavel Davidson, Martti Kirkko-Jaakkola, and Helena Leppäkoski. Inertial sensors and their applications. In Shuvra S. Bhattacharyya, Ed F. Deprettere, Rainer Leupers, and Jarmo Takala, editors, *Handbook of Signal Processing Systems*, pages 69–96. Springer New York, 2013. ISBN 978-1-4614-6858-5. doi: 10.1007/978-1-4614-6859-2_3. URL http://dx.doi.org/10.1007/978-1-4614-6859-2_3.

[2] Alberto Olivares Vicente and Kai Bötzel. *GaitWatch User Manual*.

[3] Juansempere. Wikimedia Commons File: Taitbrianzyx.svg. URL http://commons.wikimedia.org/wiki/File:Taitbrianzyx.svg. [Accessed 31 March, 2015].

[4] T.R. Bennett, R. Jafari, and N. Gans. Motion Based Acceleration Correction for Improved Sensor Orientation Estimates. In *2014 11th International Conference on Wearable and Implantable Body Sensor Networks (BSN)*, pages 109–114, June 2014. doi: 10.1109/BSN.2014.17.

[5] Simon Haykin. *Adaptive filter theory*. Prentice Hall, Upper Saddle River, N.J, 2002. ISBN 9780130484345.

[6] Peter S. Maybeck. *Stochastic Models, Estimation and Control: Volume 1*. Academic Press, 1979. ISBN 9780124110427.

[7] Wee-Soon Yeoh, I. Pek, Yi-Han Yong, Xiang Chen, and A.B. Waluyo. Ambulatory monitoring of human posture and walking speed using wearable accelerometer sensors. In *Engineering in Medicine and Biology Society, 2008. EMBS 2008. 30th Annual International Conference*

of the IEEE, pages 5184–5187, Aug 2008. doi: 10.1109/IEMBS.2008. 4650382.

[8] Alberto Olivares Vicente. *Signal Processing of Magnetic and Inertial Sensor's Signals applied to Human Body Motion Monitoring*. PhD thesis, University of Granada, Granada, January 2013. URL `http://hera. ugr.es/tesisugr/21910947.pdf`.

[9] P.H. Veltink, H.B.J. Bussmann, W. de Vries, Wim L.J. Martens, and R.C. van Lummel. Detection of static and dynamic activities using uniaxial accelerometers. *Rehabilitation Engineering, IEEE Transactions on*, 4(4):375–385, Dec 1996. ISSN 1063-6528. doi: 10.1109/86.547939.

[10] B. Najafi, K. Aminian, A. Paraschiv-Ionescu, F. Loew, C.J. Bula, and P. Robert. Ambulatory system for human motion analysis using a kinematic sensor: monitoring of daily physical activity in the elderly. *Biomedical Engineering, IEEE Transactions on*, 50(6):711–723, June 2003. ISSN 0018-9294. doi: 10.1109/TBME.2003.812189.

[11] M. Ermes, J. Parkka, J. Mantyjarvi, and I. Korhonen. Detection of daily activities and sports with wearable sensors in controlled and uncontrolled conditions. *Information Technology in Biomedicine, IEEE Transactions on*, 12(1):20–26, Jan 2008.

[12] O. Giggins, D. Kelly, and B. Caulfield. Evaluating rehabilitation exercise performance using a single inertial measurement unit. In *Pervasive Computing Technologies for Healthcare (PervasiveHealth), 2013 7th International Conference on*, pages 49–56, May 2013.

[13] J. Lupinski, V. Menon, P. Roh, S. Yuen, A. Valdevit, and J. Andrish. Measuring knee compliance to facilitate post-op ligament rehabilitation. In *Bioengineering Conference (NEBEC), 2011 IEEE 37th Annual Northeast*, pages 1–2, April 2011. doi: 10.1109/NEBC.2011.5778529.

[14] V. Bonnet, C. Mazza, P. Fraisse, and A. Cappozzo. Real-time estimate of body kinematics during a planar squat task using a single inertial measurement unit. *Biomedical Engineering, IEEE Transactions on*, 60 (7):1920–1926, July 2013. ISSN 0018-9294. doi: 10.1109/TBME.2013. 2245131.

[15] Rui Zhang, F. Hoflinger, and L. Reindl. Inertial sensor based indoor localization and monitoring system for emergency responders.

Sensors Journal, IEEE, 13(2):838–848, Feb 2013. ISSN 1530-437X. doi: 10.1109/JSEN.2012.2227593.

[16] T. Bennett, R. Jafari, and N. Gans. An extended kalman filter to estimate human gait parameters and walking distance. In *American Control Conference (ACC), 2013*, pages 752–757, June 2013. doi: 10. 1109/ACC.2013.6579926.

[17] eMarketer. 2 Billion Consumers Worldwide to Get Smart(phones) by 2016. URL `http://www.emarketer.com/Article/ 2-Billion-Consumers-Worldwide-Smartphones-by-2016/1011694`.

[18] Apple Inc. ResearchKit. URL `http://www.apple.com/researchkit`. [Accessed 20 March, 2015].

[19] The Michael J. Fox Foundation for Parkinson's Research (MJFF) and Intel Corporation. The Michael J. Fox Foundation and Intel Join Forces to Improve Parkinson's Disease Monitoring and Treatment through Advanced Technologies. URL `http://goo.gl/PxQAof`. [Accessed 20 March, 2015].

[20] SparkFun Electronics. *IMU Analog Combo Board 5DOF*, . URL `https: //www.sparkfun.com/products/retired/9268`. [Accessed 17 March 2015].

[21] SparkFun Electronics. *Gyro Breakout Board IDG500*, . URL `https: //www.sparkfun.com/products/retired/9094`. [Accessed 17 March 2015].

[22] Analog Devices. *ADXL335: Small, Low Power 3-Axis ±3G Accelerometer*, . URL `http://www.analog.com/en/mems-sensors/ mems-inertial-sensors/adxl335/products/product.html`. [Accessed 17 March 2015].

[23] Analog Devices. *ADXL345: 3-Axis, ±2g/±4g/±8g/±16g Digital Accelerometer*, . URL `http://www.analog.com/en/mems-sensors/ mems-inertial-sensors/adxl345/products/product.html`. [Accessed 17 March 2015].

[24] InvenSense. *IMU-3000 Triple Axis MotionProcessor™Gyroscope*. URL `http://www.invensense.com/mems/gyro/imu3000.html`. [Accessed 17 March 2015].

[25] SparkFun Electronics. *MicroMag 3-Axis Magnetometer*, . URL `https://www.sparkfun.com/products/retired/244`. [Accessed 17 March 2015].

[26] ALVIDI. *AVR ATxmega – Development Module*. URL `http://www.alvidi.de/avr_xmodul_en.html`. [Accessed 17 March 2015].

[27] J.R. Raol. *Multi-Sensor Data Fusion with MATLAB®*. CRC Press, 2009. ISBN 9781439800058. URL `https://books.google.de/books?id=7s8xpR-5rOUC`.

[28] Rudolph Emil Kalman. A new approach to linear filtering and prediction problems. *Transactions of the ASME–Journal of Basic Engineering*, 82(Series D):35–45, 1960.

[29] Gregory F. Welch. Kalman filter. In Katsushi Ikeuchi, editor, *Computer Vision*, pages 435–437. Springer US, 2014. ISBN 978-0-387-30771-8. doi: 10.1007/978-0-387-31439-6_716. URL `http://dx.doi.org/10.1007/978-0-387-31439-6_716`.